

L_{23} soft-x-ray emission and absorption spectra of Na

T. A. Callcott* and E. T. Arakawa

Health and Safety Research Division, Oak Ridge National Laboratory, Oak Ridge, Tennessee 37830

D. L. Ederer

Synchrotron Ultraviolet Radiation Facility, National Bureau of Standards, Washington, D. C. 20234

(Received 10 July 1978)

The L_{23} soft-x-ray emission (SXE) and soft-x-ray absorption (SXA) edges have been measured. The SXE edges were measured at temperatures between 85 and 380 K, and analyzed to obtain edge positions and widths. The widths increased from $\Gamma_{\text{SXE}} = 100$ meV at 85 K to 150 meV at 320 K and to 180 meV above the melting point at 380 K. Both SXE and SXA edges were measured at 100 K with the same spectrometer, and the data were analyzed to obtain values of the edge widths ($\Gamma_{\text{SXE}} = 100$ meV and $\Gamma_{\text{SXA}} = 64$ meV), of the many-body peaking parameter ($\alpha_{\text{SXE}} = 0.15$ and $\alpha_{\text{SXA}} = 0.24$), of the gap between the edges ($E_g = 74$ meV), and of the excess width of the emission edge [$(\Delta\Gamma)^2 = \Gamma_{\text{SXE}}^2 - \Gamma_{\text{SXA}}^2 = 5900$ (meV) 2]. The values of E_g and $(\Delta\Gamma)^2$ were used in the partial-lattice-relaxation theory of Almladh to obtain a value of the core-hole lifetime broadening ($\Gamma_p = 10$ meV). We conclude that structure in the transition density of states, many-body effects, and lattice relaxation all have important effects on the edge structure, and suggest that rounding of the SXE edge by partial relaxation accounts for the smaller peaking parameter obtained from the SXE data as compared to the SXA data.

I. INTRODUCTION

Soft-x-ray emission (SXE) and soft-x-ray absorption (SXA) edges in simple metals have been extensively analyzed for the information they can provide about a variety of physical processes occurring in solids. Originally an explanation of the edge shape was sought in terms of electric-dipole transitions of an electron between an atomic core level and nearly free-electron conduction-band levels. In the last decade, there has been extensive discussion by many workers of the effects of many-body processes on the edges.¹⁻⁶ Much attention has also been paid to broadening processes affecting the core levels.^{5,7-9} Recent work indicates that the phonon-core-hole interaction is the dominant broadening mechanism affecting the core levels and the experimentally observed edge widths.⁷⁻¹¹ Moreover, it has become clear from the work of Almladh and Mahan that the dynamical aspects of this interaction, due to partial relaxation of the lattice about the core hole before emission, may have a very large effect on the shape of the emission edge.^{10,11}

The SXE spectra of Na obtained by a number of workers between 1940 and 1970 have been reviewed by McAlister.¹²⁻¹⁹ The SXA spectra have been measured by Kunz and co-workers at DESY.²⁰ The absorption data were analyzed by Dow and Sonntag to obtain values of the edge width and of α , a parameter which characterizes the effect of many-body processes on the $L_{2,3}$ edges.⁴ These effects are discussed further below. Very recently Crisp has published a careful study of

the effects of self-absorption on the emission edge.¹⁹ His results are important because self-absorption has frequently been invoked to explain away anomalous features of the SXE spectra.¹⁰

In this paper, we report measurements of both the L_{23} SXE and SXA spectra of Na. The data are novel in several respects, though we have published the results of a similar set of measurements for Li elsewhere.²¹ Of greatest importance perhaps are the measurements of both the emission and absorption edges with the same spectrometer. This allows the widths of the edges and the separation between them to be accurately measured without questions about the relative resolutions and energy calibrations of the spectrometers used for the two sets of measurements. These data are critical for the analysis of partial relaxation effects using the Almladh-Mahan theory. We have also measured the breadth and position of the emission edge at a series of temperatures between 80 and 400 K; the latter temperature is above the melting point. These data provide information about the temperature dependence of the core level widths which may be compared to similar information obtained from studies of x-ray photoemission and from measurements of the temperature dependence of the shape of the absorption edge. Finally, we present SXE and SXA spectra extending to several electron volts on either side of the respective edges, which is useful for assessing the effects of band structure on the x-ray spectra.

In a first approximation, the theoretical description of the L_{23} x-ray spectra can be given in

terms of one-electron electric-dipole transitions between $2p$ core states and s - and d -like conduction-band states. Gupta and Freeman have calculated the one-electron spectra expected including the effects of band structure on both the density of states and on the transition-matrix elements.²² As will be discussed below, the band structure produces important structure in the spectra away from the band edge but does not add structural features within a few tenths of an eV from the band edge where the data are analyzed for evidence of many-body effects and core-hole broadening.

Many-body processes have an important effect on the x-ray spectra of simple metals. Very near the spectral edge, the complex expression obtained from the many-body theory is dominated by a term of the form $(E - E_F)^{-\alpha}$, where α is given by the many-body analysis of Nozieres *et al.*² When α is negative, this term rounds off the edges and, when positive, causes a peaking at the spectral edge. For Na both the emission and the absorption spectra are sharply peaked near their edges. We analyze this peaking to obtain values of α for comparison with theory.

Many broadening processes effect the observed width of the edges. Among these are phonon broadening of the Fermi edge and core level and lifetime broadening of the core level. The observed temperature dependence of the edge width and recent calculations of Hedin and Flynn indicate that phonon broadening of the core level is the dominant broadening mechanism for the absorption spectra.^{8,9} Almladh¹⁰ and Mahan¹¹ have recently published calculations that suggest that additional phonon-core level effects are observed for the emission spectra when the core hole lifetime is comparable to the lattice relaxation time so that partial relaxation of the lattice about the core hole occurs before the emission event. In Li this partial relaxation accounts for the premature peak and shoulder observed in the SXE edge.^{10,11,21} Here we will argue that the partial relaxation theory accounts in a satisfactory manner for the excess width observed for the emission spectrum and for the observed gap between the emission and absorption edges. It also allows us to derive a value of the core-hole lifetime from our data.

Since the phonon broadening of the core level may be described by a Gaussian function and since this is the dominant broadening factor effecting the edges, we have folded a Gaussian broadening function with the single electron transition edge spectra and the many body peaking factor in order to fit the data within a few tenths eV from the SXE and SXA edges. The expression used to fit

the edges was

$$I(E, \alpha, \gamma) = \frac{1}{\sqrt{2\pi}} \int_{-\infty}^{\infty} I_0(E')(E' - E_F)^{-\alpha} \times \exp\left[-\frac{1}{2}\left(\frac{E - E'}{\gamma}\right)^2\right] dE',$$

where $I_0(E')$ is the single-electron edge spectrum, $(E' - E_F)^{-\alpha}$ is the many-body peaking factor, and γ is related to the full width at half maximum (FWHM) value of the Gaussian by $\Gamma_{1/2} = \sqrt{8 \ln 2} \gamma = 2.355 \gamma$.

The effects of α and $\Gamma_{1/2}$ on a step-function edge are illustrated in Fig. 1. In Fig. 1(a), $I(E - E_F, \alpha, \Gamma_{1/2})$ is plotted for $\alpha = 0.25$ and a range of values for $\Gamma_{1/2}$ from 0.06 to 0.12 eV. In practice the data were analyzed with the spectra normalized to the spectral maximum. The data of Fig. 1(a) is replotted in Fig. 1(b) renormalized in this fashion. For a given value of α , varying $\Gamma_{1/2}$ clearly

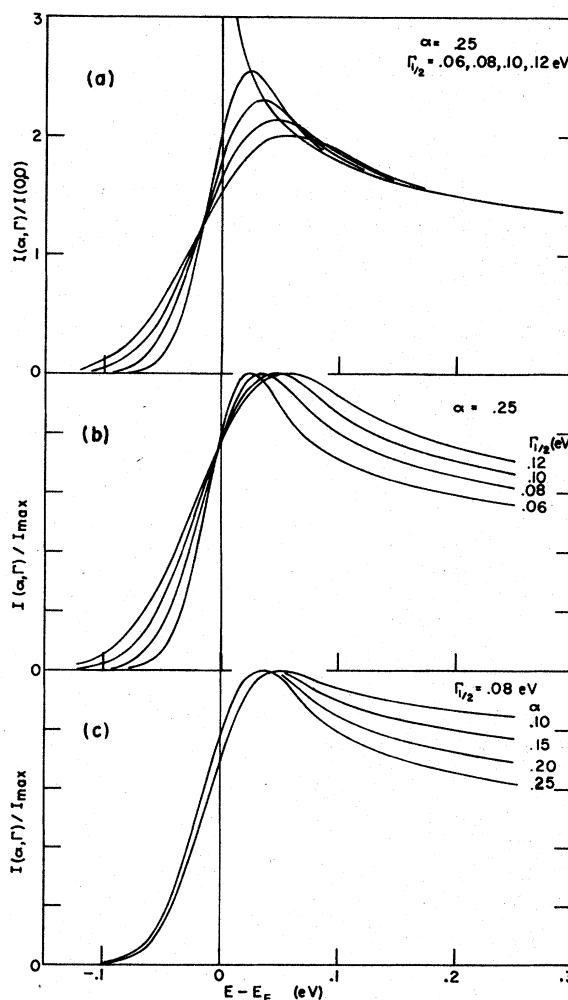


FIG. 1. Effect of many-body parameter (α) and Gaussian half-width ($\Gamma_{1/2}$) on x-ray edge spectra.

effects both the edge shape and the shape of the spectral curves beyond the spectral maximum. In Fig. 1(c) curves of I/I_{\max} are plotted for a single broadening factor $\Gamma_{1/2} = 0.08$ eV and for a range of peaking factors, α , between 0.10 and 0.25. Variations of α over this wide range has only a small effect on the edge width but strongly affects the shape of the curve beyond the peak maximum. Because of the small effect of α on the edge width, we analyzed the data by first fitting the leading edge by varying $\Gamma_{1/2}$ with an approximate value of α and then by varying α to fit the shape of the curve beyond the spectral maximum.

Several features of the curves of Fig. 1 are important for the analysis of the data. First the edge widths determined are nearly independent of the origin or magnitude of the peaking factor. Second, the position of the Fermi edge is not at the point of maximum slope of the edge but is substantially displaced toward the peak maximum. This fact has a large effect on the value we obtain for the separation between the SXE and SXA edges. Finally, an analysis of curves like those of Fig. 1(b) with constant α and various values of $\Gamma_{1/2}$ shows that both the position of the edge and its experimental width $\Gamma_{1/2}$ can be determined without a detailed computer fit of each curve. In interpreting the data for the temperature dependence of the emission edge width, we used the 10%–90% width of the edge to determine $\Gamma_{1/2}$ and the 70% point of the edge to determine the edge position. For $\alpha = 0.15$ the value of α used to fit the emission data, we find that $\Gamma_{10-90} \cong 0.9 \Gamma_{1/2}$. Also for $\alpha = 0.15$, the 70% point of the curves is very nearly independent of $\Gamma_{1/2}$ and lies 0.01 eV below the true edge position.

II. PROCEDURES AND EQUIPMENT

The procedures and equipment used for these experiments have been described in detail elsewhere.^{21,23} We will give only a brief description of essential features here. The data were obtained in two different sets of experimental apparatus which are described separately below. The temperature dependence of the emission spectra were measured in an UHV chamber at the Oak Ridge National Laboratory (ORNL). In these experiments, Na was evaporated onto a Cu anode which was cooled by circulating coolant (liquid nitrogen, methanol cooled by dry ice, ice water, and compressed air). The temperature was monitored by a thermocouple clamped to the emitting surface. A 4–6-mA beam of 2–2.5 keV electrons was incident at 45° to the anode surface. Soft x rays emitted normally from the surface were measured using a 2-m grazing incidence mono-

chromator fitted with a 1200 lines/mm grating and a channeltron detector. The monochromator was calibrated against the line spectra produced by a condensed spark discharge in air. The resolution cited for these data was determined by measuring the actual line widths observed for narrow single lines in the spark spectra.

Measurements of the SXA spectra and of the SXE spectra measured to establish the edge separation were made at the National Bureau of Standards (NBS) electron storage ring. Absorption measurements were made with thin Na films evaporated onto 1000-Å Al substrates supported on Ni mesh. Absorption coefficients were determined from measurements of the transmission of the Al substrate with and without the Na film. The absorption films were mounted on a holder which also had a Cu emitting anode which could be moved into the beam line so that it faced the spectrometer. A 5-mA beam of 2.5 keV electrons was used to excite the emission spectra from a Na film evaporated onto the Cu emitter. Transmitted synchrotron light from the storage ring and normally emitted radiation from the emission anode were both analyzed using the same 3-m grazing incidence spectrometer which was fitted with a 600 lines/mm gold grating and a channeltron detector. The spectrometer was calibrated before and after each experimental run using a gas absorption cell filled with Ar or He which have lines bracketing the region of experiment interest. In Ar the single-electron excitations $3s3pS_0 \rightarrow 3s3p^6np^1P_1$ were used in first order, and in He the two-electron excitations $1s^2^1S_0 \rightarrow 2s2p^1P_1$ and $1s^2^1S_0 \rightarrow (+2,3)^1P_1$ were used in second order.^{24,25}

III. EXPERIMENTAL RESULTS

In Figs. 2, 3, and 5 we plot SXE data for Na. Figure 2 shows edge data taken at 85 ± 5 K at

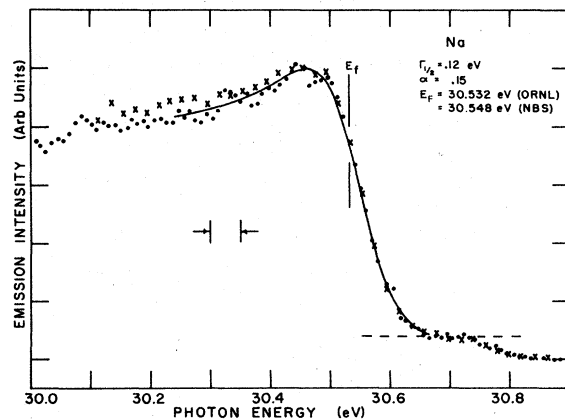


FIG. 2. SXE spectrum for Na at 85 K. Dots indicate ORNL data; crosses indicate NBS data.

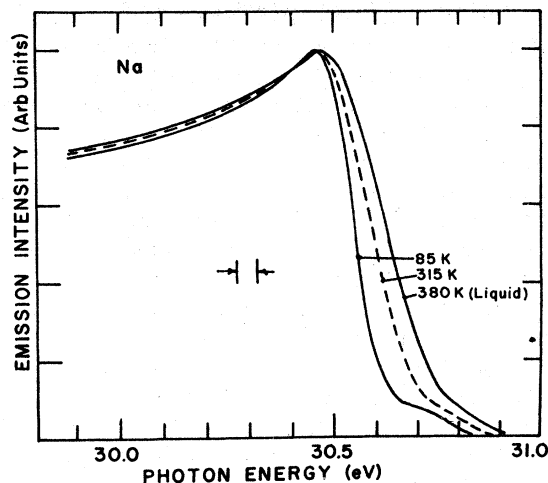


FIG. 3. SXE spectra for Na between 85 K and the melting point.

ORNL (dots) and at 100 ± 10 K at NBS (crosses). The difference in temperature results from the more efficient cooling geometry used in the ORNL apparatus. The energy scale for the figure is that given by the calibration of the ORNL spectrometer. In Fig. 2 the NBS data has been shifted to lower energies by 0.016 eV so that the two edges are superimposed. The 0.016 eV energy shift represents primarily the difference in the calibrations of the ORNL and NBS spectrometers, though up to 20% may be due to the temperature differences. The ORNL data represents the sum of 15 runs at 5 mA and 2.0 keV and the NBS data the sum of 10 runs at 5 mA and 2.5 keV. The solid line is a fit of the ORNL data using values of E_F , α , and $\Gamma_{1/2}$ shown in the inset of Fig. 2. The experimentally measured broadening of the edge given by $\Gamma_{1/2}$ may be corrected for instrumental broadening of 0.06 eV to obtain the true emission edge width Γ_{SXE} . To a good approximation, for Gaussian broadening, $\Gamma_{SXE}^2 = \Gamma_{1/2}^2 - (0.6)^2$ so that $\Gamma_{SXE} = 0.104 \pm 0.010$ eV, where the error limits were obtained from uncertainties derived from the fitting procedure and an estimate of modification of the edge shape by self-absorption.

In Fig. 2 the curve was fitted to the portion of the emission data above the dashed line. The shoulder in the data below this line is the L_2 emission peak which is strongly depressed below the L_3 peak by Koster-Kronig transitions and self-absorption. In Koster-Kronig transitions the more tightly bound L_2 level is filled by non-radiative transitions from the L_3 level with excess energy being carried off by the excitation of a conduction-band electron. According to the recent work by Crisp,¹⁹ self-absorption also has an important effect on the L_2 peak when 2.5-keV

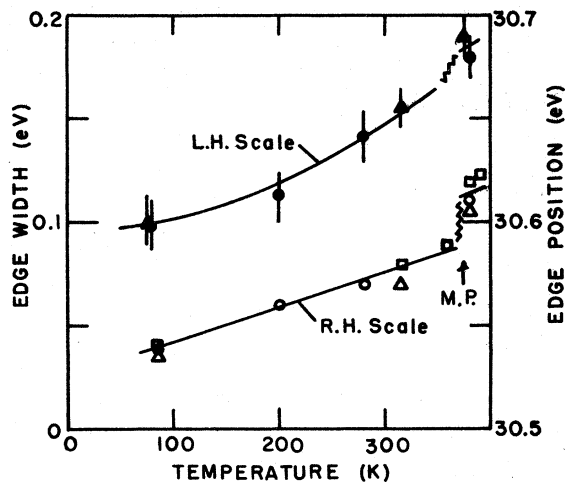


FIG. 4. Temperature dependence of the edge width and the edge position for the Na emission spectra.

electrons are used for excitation. The self-absorption has little effect, however, on the L_3 edge where the overlap from the absorption edge is much weaker but might result in a slight underestimate of the emission edge width.

In Fig. 3 emission data are plotted which were taken at temperatures between 85 K and the melting point of Na. Clearly, the edge broadens and shifts to higher energy with increasing temperature. Information taken from these curves and others like them were used to plot the temperature dependences of the SXE edge width and edge position shown in Fig. 4. Data represented by Δ were taken with a resolution of 0.06 eV, by \circ with a resolution of 0.10 eV and by \square with a resolution of 0.20 eV. Edge widths plotted are taken from the higher-resolution data only (0.06 and 0.10 eV) and are corrected for instrumental resolution. The 0.20-eV data was used primarily for determining the position of the edge near the melting point.

The curves labeled experiment in Fig. 5 are plots of the complete L_{23} emission spectrum of Na made with an instrumental resolution of 0.2 eV. This low resolution was used in order to obtain the emission spectrum in one pass. The data shown was taken at 310 K on a film evaporated at 80 K and subsequently warmed up. The data for the curve with the less prominent peak was taken shortly before the film was melted. The other curve was taken after the film was melted and re-cooled at 310 K. The overall intensity observed after melting was about 20% smaller than before melting. The film appeared shinier after melting which suggests that the change in intensity accompanied a decrease in the surface area upon melting. The two sets of data are shown here to il-

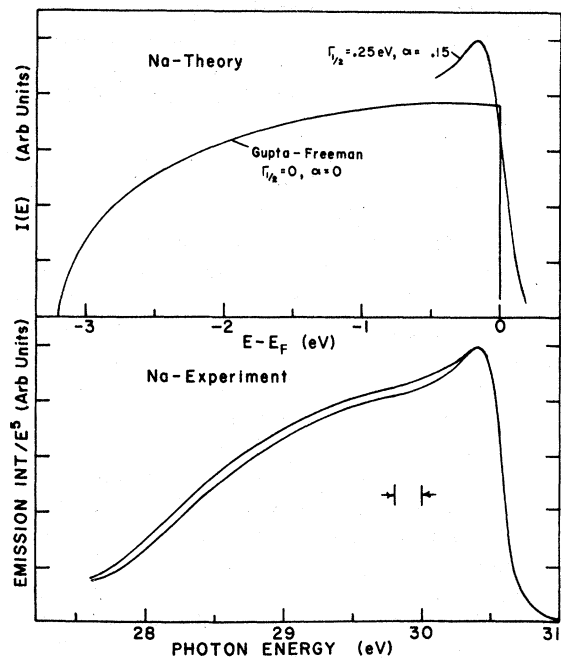


FIG. 5. Comparison of the Na emission spectrum with theory.

illustrate the range of variation of the peak near the emission edge observed in our experiments. The similar degree of variation between the NBS and ORNL data in Fig. 2 can perhaps be attributed to a difference in the roughness of the samples. The sharpest peaks observed with the cleanest and most specularly reflecting film could be fitted with a peaking factor of 0.15 ± 0.02 eV, while a value of $\alpha = 0.12$ would be necessary to fit the lower contrast peak.

In Fig. 5 the total intensity detected has been divided by E^5 to give a spectral distribution that can be more accurately compared to the one electron density of states $[I(E)]$. A factor of E^3 is included to adjust for a frequency factor appearing in the dipole matrix elements. An additional factor of E^2 adjusts for the fact that the spectrometer used has a constant wavelength resolution rather than a constant energy resolution. In the curve labeled theory in Fig. 5 the one-electron transition density of states obtained by Gupta and Freeman²² is plotted along with an edge shape obtained with $\Gamma_{1/2} = 0.25$ eV and a peaking factor of $\alpha = 0.15$. These values satisfactorily reproduce the shape of the emission edge obtained in the measurements. Since $\Gamma_{1/2}$ is a parameter that contains both the instrumental band width and the emission edge width, the large $\Gamma_{1/2}$ value required to fit the data shown in Fig. 5 just reflects the lower resolution that was used in those measurements. For $h\nu < E_F$, the Gupta and Freeman calculation qualita-

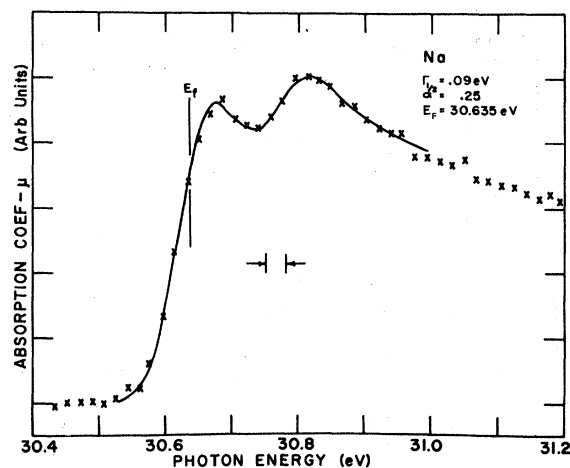


FIG. 6. SXA spectrum for Na at 100 K.

tively accounts for the shape of the measured emission spectrum except that the calculated emission spectrum is about 0.5 eV wider than that experimentally observed. To make the comparison of the spectral widths, the concave downward portion of the experimental spectrum may be fitted with a curve of the form $(E - E_t)^{1/2}$ and extrapolated to a threshold at E_t . The tailing of the emission spectrum to lower energies results from Auger processes and other inelastic processes and is a feature common to all emission spectra.

Absorption spectra of Na are plotted in Figs. 6–8. These data are taken from two sets of measurements, each of which is somewhat flawed, but which taken together satisfactorily characterize the absorption behavior of Na. In the calibration run made after taking the data of Figs. 6 and 8, we found an error in the energy calibration which was traced to a problem in the mechanical drive of the spectrometer's output slit assembly which changed the wavelength calibration and reduced the resolution from a nominal value of 0.01 eV to an actual value of 0.05–0.06 eV. However, the transmission data was optimum in that the maximum reduction of transmitted intensity above the absorption edge was about 60%. Thus, the shape of the absorption spectra for $h\nu > E_F$ would not be much influenced by scattered light. This was very important for the determination of α from the data of Fig. 6 and for the comparison to the one electron theory of Gupta and Freeman made in Fig. 8, where the shape of the absorption spectrum above the edge is important. The absorption data in Fig. 7(a), on the other hand, was taken after the spectrometer was adjusted and recalibrated, so that both the energy scale and the resolution were accurately known. This data was

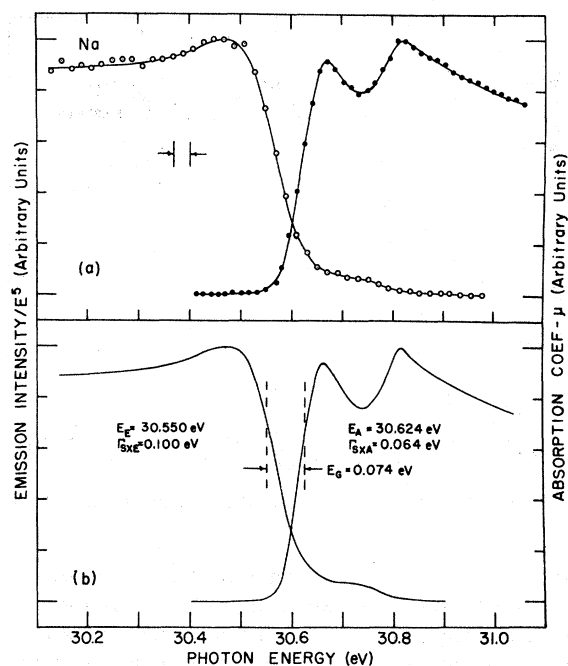


FIG. 7. SXE and SXA spectra obtained with the same spectrometer, which were used for comparison with the partial lattice relaxation theory. (a) Spectral curves fit to original data. (b) Spectral curves after correction for instrumental broadening.

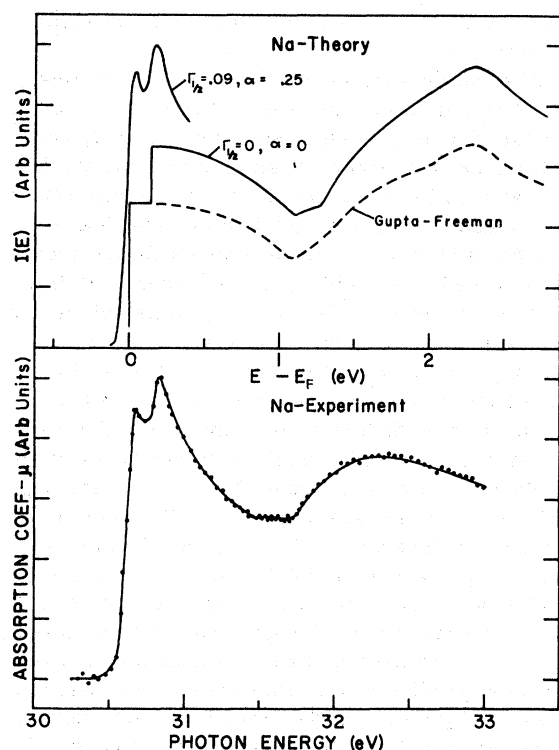


FIG. 8. Comparison of the Na absorption spectrum with theory.

used to determine the position and width of the absorption edge. However, the transmission of this film above the edge was only 2%–3%, so that small amounts of scattered light distorted the true shape of spectra for $h\nu > E_F$. This distortion produces a systematic error in the determination of α . In our analysis of the absorption spectrum, we have combined results from the two sets of spectra. The absorption edge width and position have been determined from data on the thicker film for which the resolution and energy scale are accurately known. The many body parameter α , which is not sensitive to energy calibration, was obtained from data taken with the thinner film.

A large number of parameters effect the shape of the absorption edge in Fig. 6. In addition to $\Gamma_{1/2}$ and α , the spin orbit splitting between the L_2 and L_3 levels, and relative probabilities of transitions to these levels effect the edge shape. The spin-orbit splitting was taken as 0.155 ± 0.005 eV from optical data on Na vapor. $\Gamma_{1/2}$ was determined to be 0.09 ± 0.01 eV from the initial rise of the absorption edge. As discussed earlier, the value obtained in this way is nearly independent of the values assumed for the other parameters. The curve shown in Fig. 6 was obtained with values of $\alpha = 0.25$ and an L_2 to L_3 ratio of 0.37. With the same values for $\Gamma_{1/2}$ and the spin orbit splitting, a value of $\alpha = 0.22$ and an L_2 to L_3 ratio of 0.35 gave a slightly less satisfactory fit to the absorption data. We concluded that a value of $\alpha = 0.24 \pm 0.04$ would fit the data for any plausible values of the other fitting parameters.

If pure $j-j$ coupling existed between the core hole and the electron excited into the conduction band, the intensity ratio between the L_3 and the L_2 edges would be 2:1. However, Onodera²⁶ has suggested that because the exchange energy is about a factor of two greater than the spin-orbit splitting the coupling would be intermediate between $j-j$ and LS and the intensity ratio of the L_3 and the L_2 edges would not be 2:1. This result is consistent with our measurements and those of the DESY group who have reported a similar value of the L_2 - L_3 ratio.

In Fig. 7(a) we plot both the SXA and SXE edges obtained with the NBS spectrometer. Since we wished to use this data to make a careful comparison of the relative widths of the SXE and SXA edges, we used a deconvolution procedure to remove the effects of the instrument broadening from the data. The instrument broadening function was approximated as a Gaussian of half width 0.42 \AA , and the deconvolutions were performed on the experimental intensities before conversion to I/E^5 for the SXE data and to $\ln(I_0/I)$ for the SXA data. Curves fit to the original data are

TABLE I. Values of physical parameters derived from analysis of SXE and SXA spectra.

Emission	
Edge position (E_E)	30.532 (85 K, ORNL calibration)
	30.550 (100 K, NBS calibration)
Edge width (Γ_{SXE})	100 \pm 10 meV (85 K)
Peaking parameter (α_B)	0.15 \pm 0.03
Absorption	
Edge position (E_A)	30.624 (NBS calibration)
Edge width (Γ_{SXA})	64 \pm 5 meV (100 K)
Peaking parameter (α_A)	0.24 \pm 0.04
L_2/L_3 ratio	0.37 \pm 0.03
Spin-orbit splitting	155 \pm 5 meV
Emission and absorption features	
Gap between edges (E_g)	74 \pm 10 meV
$\Gamma_{SXE}^2 - \Gamma_{SXA}^2 = \Delta\Gamma^2$	5900 \pm 1000 meV ²
Core-hole lifetime (Γ_{2p})	10.5 \pm 1.0 meV

shown in Fig. 7(a). The results after deconvolution are shown in Fig. 7(b). The Fermi edge position for the absorption spectrum was found at $E_A = 30.624 \pm 0.005$ eV and the edge width to be $\Gamma_{SXA} = 0.100 \pm 0.005$ eV. These values of E_E and Γ_{SXE} obtained after the deconvolution are slightly different, but well within the error limits quoted for estimates obtained without the deconvolution analysis in Fig. 2. The separation between the edges is $E_g = 0.074 \pm 0.010$ eV. We emphasize again that the true magnitude of this gap can only be obtained after the effect of broadening on a peaked edge shape is properly taken into account. The parameters that we have obtained from our data for both the emission and absorption edges are summarized in Table I.

In Fig. 8 we plot an absorption spectrum (shown as points with a solid curve drawn through the points to guide the eye) extending to 2.5 eV above the absorption edge and compare it to theoretical curves based on the calculations of Gupta and Freeman. The dashed curve in the figure is taken from the transition density of states calculated by Gupta and Freeman for transition from a single p level to s and d like states in the conduction band. The solid curve, labeled $\Gamma_{1/2} = 0$, $\alpha = 0$, represents the unbroadened contribution from two p levels separated by 0.155 eV and weighted in the ratio of 0.4 to 1. The curve labeled $\Gamma_{1/2} = 0.09$ eV, $\alpha = 0.25$ is the same curve when modified by the

peaking function $(E - E_A)^{-\alpha}$ and the Gaussian broadening function of half width $\Gamma_{1/2}$.

Some features of the observed SXA spectrum clearly result from the effects of band structure on the one-electron spectrum and are qualitatively explained by the calculations. The continued decrease of the spectrum for 1 eV above the edge and the double minimum in the observed spectrum reflect the decrease in the s -like part of the conduction band density of states to a minimum when the conduction band contacts the Brillouin-zone boundary. The double minimum in the calculated spectrum falls about 0.2 eV above the same feature in the experimental spectrum. Thus the energy of the calculated SXA spectrum, like that of the calculated SXE spectrum, would have to be compressed to give a really good fit to the data.

The very sharp peaking of the SXA spectrum at the edge cannot be explained by band structure effects since the one electron transition density of states is very nearly flat at the edge and changes slowly over an energy range of the order of 0.10 eV. The most satisfactory current explanation for the peaks is provided by many body theory.

In Fig. 9 we have plotted the first and second moments of the core-hole broadening spectrum of Na calculated by Almbladh for partial relaxation effects. The abscissa represents the reciprocal of the core-hole lifetime in energy broadening units of millielectron-volts. The dashed

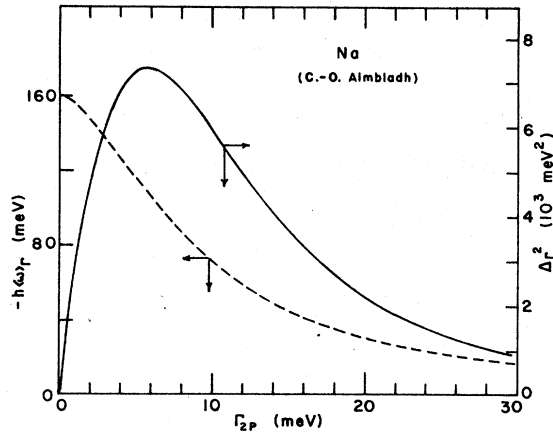


FIG. 9. Dependence on core-hole lifetime of the first and second moments of the core-hole broadening produced by partial lattice relaxation. Curves adapted from Ref. 10. Arrows indicate values of core-hole lifetime derived from measurements of the gap between the x-ray edges (left-hand scale) and from excess broadening of the emission spectrum (right-hand scale).

curve and left-hand ordinate represent the first moment or centroid of the distribution and thus relates the shift in the energy position of the emission edge as a function of core-hole lifetime. For very short lifetime (large Γ_{2p}) the edge is not shifted, and for very long lifetimes (small Γ_{2p}), corresponding to a fully relaxed lattice, a maximum shift in the core-hole energy level of 160 meV is predicted. The solid curve and right-hand ordinate represent the additional width of the emission edge due to partial relaxation effects. In the experimental data, this represents the additional width $\Delta\Gamma$ of the emission edge as compared to the absorption edge calculated according to the prescription $\Delta\Gamma^2 = \Gamma_{SXE}^2 - \Gamma_{SXA}^2$.

Thus Almbladh's version of the partial relaxation theory gives us the means of obtaining two separate estimates of the core hole lifetime, the first from the observed separation between the emission and absorption edges and the second from the excess width of the emission edge. This energy shift and extra broadening are listed as E_q and $\Delta\Gamma^2$ in Table I. In Fig. 9 the experimentally determined values are indicated by arrows. The energy gap measurement gives an estimate of $\Gamma_{2p} = 10$ meV and the excess broadening an estimate of $\Gamma_{2p} = 11$ meV. This agreement is very satisfactory in view of the uncertainties in both the measurements and in the theory. A value of $\Gamma_{2p} = 10.5 \pm 1.0$ meV accounts for the uncertainties in the experimental data but does not reflect systematic shifts that may be introduced by varying the theoretical parameters.

IV. CONCLUSIONS AND DISCUSSION

We conclude from our analysis that band-structure effects, many body processes and partial relaxation effects all make important contributions to the observed SXA and SXE spectra of the L_{23} levels of Na. We note that this conclusion differs from that reached for Li where no convincing evidence for many-body effects was found in the data.

However our results present one problem of interpretation. Namely the many-body parameters derived from the SXA and SXE spectra are 0.25 and 0.15, respectively; whereas according to theory they must be the same. We do not believe that this difference reflects an experimental problem. Both sets of data were made with the same spectrometer and at the same resolution. Moreover it is not a feature common to other materials. In recent measurements of Al and Mg with the same apparatus, both SXE and SXA edges can be satisfactorily described with the same peaking function.

Two explanations of the different values of α obtained from SXA and SXE spectra seem possible. The first is that the one-electron transition density of states is decreasing more rapidly near the Fermi level than is indicated by the Gupta and Freeman calculation. This would tend to reduce the peaking of the emission edge and increase that of the absorption edge. The second explanation is suggested by the fact that the core-hole lifetime value of $\Gamma_{2p} = 10$ meV that was obtained using our data and Almbladh's theory is comparable to the lattice relaxation time for Na. For this case, the core-hole broadening is not well described by a Gaussian function but has structure that has the effect of rounding off the emission edge. In Li the suppression of the emission spectrum at the edge is clearly evident. It seems likely that a similar effect is present for Na, but that it is masked by the many-body peaking near the edge. If band-structure effects are responsible for the discrepancy between the peaking factors determined from the SXA and SXE spectra, the "true" value should lie between the values of 0.15 and 0.25 obtained by fitting the SXE and SXA data, respectively. If the discrepancy results from partial relaxation effects which modify only the emission edge, then the value of $\alpha = 0.25$ obtained from the SXA data would be the value which should be compared to many body calculations.

Our values for α the many-body parameter derived from the SXA and the SXE spectra are quite different; however the value we obtain for α_{SXA} (0.24) is in good agreement with the value (0.25) obtained by Dow using the data of the DESY group.⁴

Onodera on the other hand used his formalism to fit the DESY data and obtained a value of α_{SXA} equal to 0.41. This inconsistency we feel is more likely due to the method employed to fit the data rather than necessarily to a flaw in the formalism developed by Onodera, since Dow, using Onodera's formalism, obtained a value of α_{SXA} consistent with his earlier analysis of the DESY data.²⁷ Furthermore recent theoretical development^{27,28} suggest modifications to the formalism developed by Onodera. Further analysis of the data will have to include these recent developments.

ACKNOWLEDGMENTS

We gratefully acknowledge helpful conversations with J. D. Dow and G. D. Mahan and correspondence with C. O. Almbladh. We also thank George Rakowsky and Alex Filitovich of the National Bureau of Standards storage ring staff for their help in obtaining the data. Research sponsored jointly by the National Bureau of Standards and the Division of Biomedical and Environmental Research, U. S. Department of Energy, under Contract No. W-7405-eng-26 with the Union Carbide Corporation.

*Permanent address: Physics Dept., University of Tennessee, Knoxville, Tenn. 37916.

¹G. D. Mahan, Phys. Rev. **163**, 612 (1967).

²P. Nozières and G. T. DeDominicis, Phys. Rev. **178**, 1097 (1969); also B. Roulet, J. Gavoret, and P. Nozières, Phys. Rev. **178**, 1072 (1969); **178**, 1084 (1969).

³G. D. Mahan, in *Solid State Physics*, edited by H. Ehrenreich, F. Seitz, and D. Turnbull (Academic, New York, 1974), Vol. **29**, pp. 75–138. This review article summarizes work through 1973.

⁴J. D. Dow and B. F. Sonntag, Phys. Rev. Lett. **31**, 1461 (1973).

⁵J. D. Dow, Phys. Rev. B **9**, 4165 (1974); J. D. Dow, J. E. Robinson, J. H. Slowik, and B. F. Sonntag, B **10**, 432 (1974); J. D. Dow and D. R. Franceschetti, Phys. Rev. Lett. **34**, 1230 (1975).

⁶P. H. Citrin, G. K. Wertheim, and Y. Baer, Phys. Rev. Lett. **35**, 885 (1975).

⁷A. J. Glick and A. L. Hagen, University of Maryland Technical Report No. 76-121, 1976, pp. 76–278 (unpublished).

⁸Lars Hedin and A. Rosengren, J. Phys. (to be published).

⁹C. P. Flynn, Bull. Am. Phys. Soc. **22**, 320 (1974); also Phys. Rev. Lett. **37**, 1445 (1976).

¹⁰C. O. Almbladh, Solid State Commun. **22**, 339 (1977); also Phys. Rev. B **16**, 4343 (1977).

¹¹G. D. Mahan, Phys. Rev. B **15**, 4587 (1977).

¹²H. W. B. Skinner, Trans. Soc. Lond. A **239**, 95 (1940).

¹³W. M. Cady and D. H. Tomboulion, Phys. Rev. **59**, 389 (1941).

¹⁴A. Sen, Indian J. Phys. **30**, 415 (1956).

¹⁵T. Sagawa, Scient. Repts. Tohoku Univ. **45**, 232 (1961).

¹⁶R. S. Crisp and S. E. Williams, Philos. Mag. **6**, 365 (1961).

¹⁷G. A. Rooke, in *Soft X-ray Band Structure and the Electronic Structure of Metals and Materials*, edited by D. J. Fabian (Academic, New York, 1968), p. 185.

¹⁸A. J. McAlister, R. C. Dobbyn, J. R. Cuthill, and M. L. Williams, in *Soft X-ray Emission Spectra of Metallic Solids*, NBS No. 369, pp. 15 and 67, 1974 (unpublished).

¹⁹R. S. Crisp, Philos. Mag. **36**, 609 (1977).

²⁰C. Kunz, R. Haensel, G. Keitel, P. Schreiber, and B. Sonntag, in *Electronic Density of States*, edited by L. H. Bennett, NBS No. 323, 275, 1971 (unpublished); also Phys. Rev. Lett. **23**, 528 (1969); also DESY Internal Report No. F41-76/03, 85, 1976 (unpublished); also DESY Report No. 70/48, 6, 1970 (unpublished).

²¹T. A. Callcott and E. T. Arakawa, Phys. Rev. Lett. **38**, 442 (1977); also Phys. Rev. B **16**, 5185 (1977).

²²R. P. Gupta and A. J. Freeman, Phys. Lett. A (Netherlands) **59**, 223 (1976).

²³National Bureau of Standards equipment, D. L. Ederer and S. Ebner, A User's Guide to SURF, NBS internal report, 1976 (unpublished); R. P. Madden, D. L. Ederer, and K. Codling, Appl. Opt. **6**, 31 (1964).

²⁴R. P. Madden and K. Codling, Astrophys. J. **141**, 364 (1965).

²⁵R. P. Madden, D. L. Ederer, and K. Codling, Phys. Rev. **177**, 136 (1969).

²⁶H. A. Bethe and E. E. Saltpeter, *Quantum Mechanics of One and Two-Electron Atoms*, (Academic, New York, 1957), pp. 292–295.

²⁷J. D. Dow (private communication).

²⁸G. D. Mahan (private communication).